CHEMISTRY
A EUROPEAN JOURNAL

COMMUNICATION

DOI: 10.1002/chem.201204160

Core–Shell AgNP@CeO_2 Nanocomposite Catalyst for Highly Chemoselective Reductions of Unsaturated Aldehydes

Takato Mitsudome,[a] Motoshi Matoba,[a] Tomoo Mizugaki,[a] Koichiro Jitsukawa,[a] and Kiyotomi Kaneda*[a, b]

In supported metal-nanoparticle (NP) catalysts, a strong metal–support interaction (SMSI) is one of the most important factors that influence the catalytic performance. Supports that affect the catalytic properties of metal NPs can be considered to be "macroligands" for the active metal NPs, and the ligand effect can be tuned by screening the supports, altering their compositions, and controlling various parameters during their preparation. However, metal NPs are often located on the surface of the supports, and the ligand effect can only take place at the interface between the bottom of the metal NPs and the surface of the supports. This implies that many sites remain on the metal NP surface with the potential to yield the ligand effect through interaction with the support. Thus, increasing such ligand interactions between metal NPs and supports will lead to superior catalytic performances over conventionally supported metal NPs.

As a new strategy for increasing the number of metal–support interaction sites, an attractive conceptual design is core–shell nanocomposite catalysts consisting active metal NPs in the core and supports in the shell.[1] The core–shell structure would be ideal for exploiting the ligand effect due to its maximized metal NP–support interface area. However, covering active core species with a shell makes it difficult for reactants to diffuse into the core, and thus the applications of core–shell catalysts to organic transformations under liquid-phase conditions are limited.[2]

We have recently reported a successful synthesis of a core–shell AgNP–CeO_2 nanocomposite (AgNP@CeO_2) consisting of AgNPs with a 10 nm diameter in the core and self-assembled, spherical CeO_2 NPs with a 3 nm diameter in the shell.[3] AgNP@CeO_2 could catalyze highly chemoselective reductions of both nitrostyrenes to aminostyrenes and epoxides to alkenes, while maintaining the C=C bonds. The nanogaps among adjacent CeO_2 NPs in the shell enabled the reactants to access the active Ag species in the core. Maximizing the interaction between AgNPs and basic sites of the CeO_2 efficiently induced the heterolytic cleavage of H_2. The resulting Ag–hydride and proton species at the interface preferred polar functional groups over C=C bonds (Scheme 1).

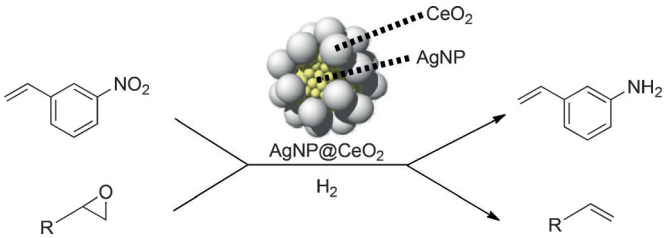

Scheme 1. Chemoselective reductions using AgNP@CeO_2.

In our continued development of unique core–shell nanocomposite catalysts, we report herein that AgNP@CeO_2 showed excellent selectivities for the chemoselective reduction of unsaturated aldehydes with H_2 to the corresponding unsaturated alcohols, which often serve as important intermediates in fragrances and pharmaceuticals.[4] Furthermore, AgNP@CeO_2 was successfully dispersed on CeO_2 (AgNP@CeO_2-D), while maintaining its core-shell structure, which led to a significant enhancement in the catalytic activity of AgNP@CeO_2. The developed AgNP@CeO_2-D catalyst afforded superior selectivity to various conventional supported metal NPs in chemoselective reductions. AgNP@CeO_2-D was also separable from the reaction mixture and reusable with the retention of its activity and selectivity.

AgNP@CeO_2 was synthesized according to our previous report.[3] The initial mole ratio of Ag to Ce (Ag/Ce) in the preparation was 1.5. The catalytic activity of AgNP@CeO_2 was examined in the hydrogenation of citral (**1**) as a model reaction in tetrahydrofuran (THF) under a pressurized H_2 atmosphere at 150 °C. The reaction proceeded efficiently to afford a mixture of the allylic alcohols geraniol and nerol (**2**) in 96 % selectivity at complete conversion, accompanied by small amounts of citronellal (**3**) and citronellol (**4**) (Table 1, entry 1).[5] Neither unsupported AgNPs nor CeO_2 alone showed any catalytic activity (entries 12 and 13), confirming the necessity of CeO_2 as a macroligand for AgNPs.

[a] Dr. T. Mitsudome, M. Matoba, Dr. T. Mizugaki, Prof. Dr. K. Jitsukawa, Prof. Dr. K. Kaneda
Department of Materials Engineering Science
Graduate School of Engineering Science, Osaka University
1-3, Machikaneyama, Toyonaka, Osaka 560-8531 (Japan)
Fax: (+81) 6-6850-6260
E-mail: kaneda@cheng.es.osaka-u.ac.jp

[b] Prof. Dr. K. Kaneda
Research Center for Solar Energy Chemistry Osaka University
1-3, Machikaneyama, Toyonaka, Osaka 560-8531 (Japan)

Supporting information for this article is available on the WWW under http://dx.doi.org/10.1002/chem.201204160.

Table 1. Reduction of citral using various catalysts.[a]

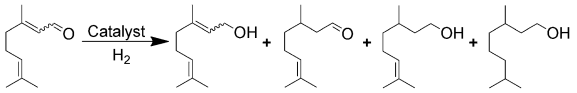

	Catalyst	t [h]	Conv. of **1** [%][b]	Sel. [%][b] **2**	**3**	**4**	**5**
1	AgNP@CeO_2 (Ag/Ce = 1.5)	72	> 99	96	1	3	0
2	AgNP@CeO_2 (Ag/Ce = 0.5)	72	21	> 99	< 1	< 1	0
3	AgNP@CeO_2 (Ag/Ce = 2.5)	72	92	88	2	10	0
4	AgNP@CeO_2-D	12	> 99	98	< 1	1	0
5	AgNPs/CeO_2	72	97	86	3	11	0
6	AuNPs/CeO_2	3	86	80	2	18	0
7	IrNPs/CeO_2	3	98	75	4	16	5
8	PtNPs/CeO_2	3	100	0	0	0	100
9	PdNPs/CeO_2	3	100	0	0	0	100
10	RhNPs/CeO_2	3	100	0	0	0	88
11	RuNPs/CeO_2	3	100	0	0	0	100
12	AgNPs	12	4	0	0	0	0
13	CeO_2	12	3	0	0	0	0

[a] Reaction conditions: Catalyst (metal: 0.008 mmol), substrate (0.25 mmol), THF (5 mL), 150 °C, H_2 (15 atm). [b] Determined by GC using an internal standard.

Interestingly, the ratio of Ag to Ce during the preparation of AgNP@CeO_2 was found to greatly affect the catalytic activity. AgNP@CeO_2 (Ag/Ce = 0.5) also exhibited high selectivity for **2**, but much lower activity than AgNP@CeO_2 (Ag/Ce = 1.5) (entry 2). On the other hand, the use of AgNP@CeO_2 (Ag/Ce = 2.5) gave a high conversion of **1**, but with lower selectivity for **2** than AgNP@CeO_2 (Ag/Ce = 1.5) (entry 3). Next, other CeO_2-supported metal NPs without a core–shell structure (metal NPs/CeO_2) were synthesized and tested in the reduction reaction under similar reaction conditions. The use of CeO_2-supported metal NPs such as Pt, Pd, Rh, and Ru resulted in undesired C=C bond hydrogenation and 3,7-dimethyloctanol (**5**) was largely formed (entries 8–11).[6] In contrast, the use of AuNPs/CeO_2 and IrNPs/CeO_2 afforded good yields of **2** (entries 6 and 7), and AgNPs/CeO_2 (entry 5) showed the best selectivity among these metal NPs/CeO_2. However, AgNPs/CeO_2 still provided a lower selectivity for **2** than AgNP@CeO_2 (entry 5 vs. 1). These results indicated that the combination of CeO_2 with AgNPs was effective and that the core–shell structure was superior to the supported one for the highly chemoselective reduction of **1** to **2**. The significant influence of the ratio of Ag to Ce in AgNP@CeO_2 on the catalysis can be explained by their geometric features. The lower activity for **1** when using AgNP@CeO_2 (Ag/Ce = 0.5) compared with AgNP@CeO_2 (Ag/Ce = 1.5) was due to the encapsulation of the core by a rich CeO_2 shell that hindered the access of **1** to the AgNPs. In the case of AgNP@CeO_2 (Ag/Ce = 2.5), scanning electron microscopy analysis (SEM) confirmed the formation of some nonencapsulated AgNPs that were active for C=C bonds, which resulted in the lower selectivity for **2**.[7]

In order to achieve a much higher catalytic performance, we next devised a highly dispersed arrangement of the AgNP@CeO_2 particles (Ag/Ce = 1.5) on inorganic supports to prevent their agglomeration. When various inorganic supports, such as Al_2O_3, TiO_2, SiO_2, hydroxyapatite, and CeO_2, were added to ethanol in the presence of AgNP@CeO_2, interestingly, AgNP@CeO_2 only adsorbed on CeO_2. Scanning transmission electron microscope (STEM) images with elemental mapping of AgNP@CeO_2 adsorbed on CeO_2 are depicted in Figure 1. Figure 1 a–c demonstrate that the Ag species were highly dispersed on CeO_2 throughout the image area. A representative high-angle annular dark-field

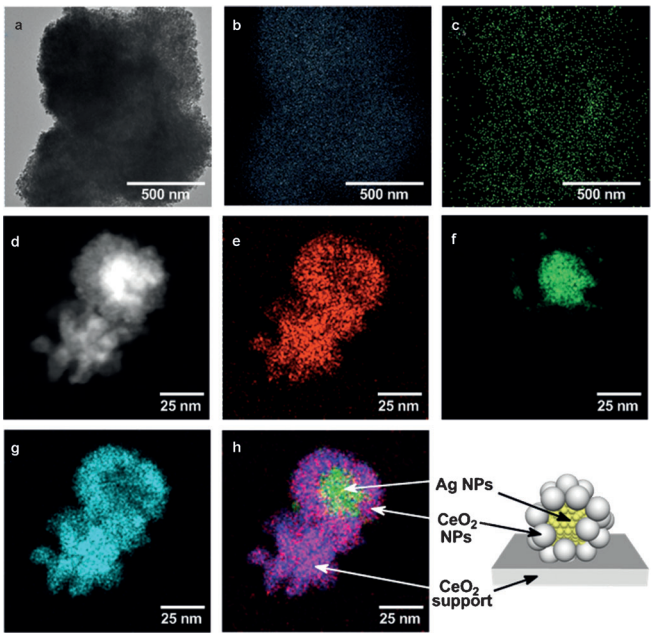

Figure 1. a) STEM images of AgNP@CeO_2-D. Elemental mapping of b) Ce and c) Ag for AgNP@CeO_2-D. d) HAADF-STEM image of AgNP@CeO_2-D. Elemental mapping of e) O, f) Ag, g) Ce, and h) their overlap for AgNP@CeO_2-D.

(HAADF) image and elemental mapping of the AgNP@CeO_2 on the surface of CeO_2 (denoted as AgNP@CeO_2-D) are shown in Figure 1 d–h. These images revealed that the original core–shell structure of AgNPs@CeO_2 was maintained.

As expected, the high dispersion led to a great enhancement in the catalytic activity of AgNP@CeO_2. Notably, AgNP@CeO_2-D showed a six times higher turnover frequency than AgNP@CeO_2 in the chemoselective reduction of **1** to **2**, while maintaining a similarly excellent selectivity to that of AgNP@CeO_2 (entry 4 vs. 1). The 98% selectivity for **2** at full conversion of **1** is higher than those of previously reported heterogeneous catalysts.[8]

With AgNP@CeO_2-D in hand, unsaturated aldehydes were extensively surveyed. AgNP@CeO_2-D was applicable for wide range of substrates (Table 2). Various aldehydes, such as terpenes (entries 1 and 5) and aliphatic (entries 6–12) and aromatic α,β-unsaturated aldehydes (entries 13–16), were efficiently converted to allylic alcohols with high selectivities. AgNP@CeO_2-D can also be applied to the hydroge-

Table 2. Chemoselective hydrogenations of unsaturated aldehydes using AgNP@CeO_2-D.[a]

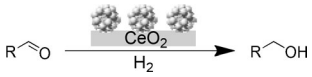

	Substrate	Product	t [h]	Conv. [%][b]	Sel. [%][b]
1	**1**	**2**	12	>99	98(94)
2[c]	**1**	**2**	12	>99	96
3[d]	**1**	**2**	12	>99	97
4			18	>99	95(90)
5			6	96	91
6	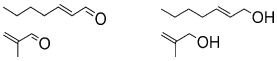		6	98	86(80)
7			24	96	81
8			12	94	92
9			8	98	92
10			6	97	92
11			15	100	92
12			3	98	94(87)
13	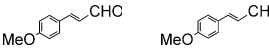		10	100	88
14			3	100	96
15			12	94	98(93)
16[e]			24	98	97
17			8	92	93
18	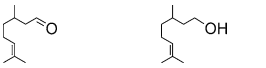		12	>99	>99(95)
19			6	>99	92

[a] Reaction conditions: AgNP@CeO_2-D (Ag: 3 mol%), substrate (0.25 mmol), THF (5 mL), 150 °C, H_2 (15 atm). [b] Determined by GC and LC using an internal standard. Values in parentheses are isolated yields. For the isolation experiments, the reactions were carried out under the following conditions. AgNP@CeO_2-D (Ag: 3 mol%), substrate (10 mmol), THF (25 mL). [c] Reuse 1. [d] Reuse 2. [e] 110 °C, H_2 (6 atm).

nation of unconjugated aldehydes. For example, 3-vinylbenzaldehyde, 5-hexenal, citronellal, and 3-cyclohexene-1-carboxaldehyde were chemoselectively hydrogenated to the corresponding alcohols (entries 17–20). Furthermore, AgNP@CeO_2-D worked well under gram-scale reaction conditions, and unsaturated alcohols were obtained in high yields (entries 1, 4, 6, 12, 15, and 18). After the reaction, AgNP@CeO_2-D was easily recovered by simple filtration and was reusable without any loss of its high efficiency (entries 2 and 3). No leaching of Ag species from AgNP@CeO_2-D was found by inductively coupled plasma (ICP) analysis. These results strongly supported the high durability of AgNP@CeO_2-D in the recycling experiments.

In conclusion, we have reported that the core–shell nanocomposite of AgNP@CeO_2 acted as an effective catalyst for the chemoselective reductions of unsaturated aldehydes to the corresponding unsaturated alcohols with H_2. The nanogaps among adjacent CeO_2 nanoparticles in the shell permitted the access of reactants to the active Ag sites in the core. Maximizing the interaction between AgNPs and the basic sites of CeO_2 successfully induced the heterolytic cleavage of H_2 to Ag–hydride and proton species, allowing the highly chemoselective reduction of unsaturated aldehydes to the corresponding allylic alcohols. Furthermore, AgNP@CeO_2 could be highly dispersed on CeO_2, exhibiting six times higher catalytic activity than the original AgNP@CeO_2 as well as a wide applicability for various substrates in the chemoselective reductions of unsaturated aldehydes. The highly dispersed AgNP@CeO_2 was also easily separable, reusable, with retention of its high catalytic performance.

Acknowledgements

This work was partially supported by a Grant-in-Aid for Young Scientists (A) from the Japan Society for the Promotion of Science (JSPS)-(23686116). T. M. thanks the Japan Association for Chemical Innovation for a grant.

Keywords: aldehydes · cerium · chemoselectivity · core–shell nanocomposite · reduction · silver nanoparticles

[1] a) C. M. Y. Yeung, K. M. K. Yu, Q. J. Fu, D. Thompsett, M. I. Petch, S. C. Tsang, *J. Am. Chem. Soc.* **2005**, *127*, 18010–18011; b) M. Cargnello, N. L. Wieder, T. Montini, R. J. Gorte, P. Fornasiero, *J. Am. Chem. Soc.* **2010**, *132*, 1402–1409 ; c) M. Cargnello, J. J. D. Jaén, J. C. H. Garrido, K. Bakhmutsky, T. Montini, J. J. C. Gámez, R. J. Gorte, P. Fornasiero, *Science* **2012**, *337*, 713–717.

[2] For core–shell catalysts possessing active species in the core for organic transformations, see: a) S. Ikeda, S. Ishino, T. Harada, N. Okamoto, T. Sakata, H. Mori, S. Kuwabata, T. Torimoto, M. Matsumura, *Angew. Chem.* **2006**, *118*, 7221–7224; *Angew. Chem. Int. Ed.* **2006**, *45*, 7063–7066; b) M. Shokouhimehr, Y. Piao, J. Kim, Y. Jang, T. Hyeon, *Angew. Chem.* **2007**, *119*, 7169–7173; *Angew. Chem. Int. Ed.* **2007**, *46*, 7039–7043; c) G. L. Li, C. A. Tai, K. G. Neoh, E. T. Kang, X. L. Yang, *Polym. Chem.* **2011**, *2*, 1368–1374; d) H. Yang, Y. Chong, X. Li, H. Ge, W. Fan, J. Wang, *J. Mater. Chem.* **2012**, *22*, 9069–9076; e) S. Wu, J. Dzubiella, J. Kaiser, M. Drechsler, X. Guo, M. Ballauff, Y. Lu, *Angew. Chem.* **2012**, *124*, 2272–2276; *Angew. Chem. Int. Ed.* **2012**, *51*, 2229–2233; f) J. Ge, Q. Zhang, T. Zhang, Y. Yin, J. Ge, Q. Zhang, T. Zhang, Y. Yin, *Angew. Chem.* **2008**, *120*, 9056–9060; *Angew. Chem. Int. Ed.* **2008**, *47*, 8924–8928; g) Y. Deng, Y. Cai, Z. Sun, J. Liu, C. Liu, J. Wei, W. Li, C. Liu, Y. Wang, D. Zhao, *J. Am. Chem. Soc.* **2010**, *132*, 8466–8473; h) X. Fang, Z. Liu, M.-F. Hsieh, M. Chen, P. Liu, C. Chen, N. Zheng, *ACS Nano* **2012**, *6*, 4434–4444; i) Y. Yang, X. Liu, X. Li, J. Zhao, S. Bai, J. Liu, Q. Yang, *Angew. Chem.* **2012**, *124*, 9298–9302; *Angew. Chem. Int. Ed.* **2012**, *51*, 9164–9168.

[3] T. Mitsudome, Y. Mikami, M. Matoba, T. Mizugaki, K. Jitsukawa, K. Kaneda, *Angew. Chem.* **2012**, *124*, 140–143; *Angew. Chem. Int. Ed.* **2012**, *51*, 136–139.

[4] a) K. Bauer, D. Garbe, H. Surburg, *Common Fragrance and Flavour Materials*, Wiley-VCH, Weinheim, **1997**; b) S. Nishimura, *Handbook of Heterogeneous Catalytic Hydrogenation for Organic Synthesis* Wiley, New York, **2001**; c) J. A. Dumesic, G. W. Huber, M. Boudart, *Handbook of Heterogeneous Catalysis, Vol. 7*, 2nd ed., Wiley-VCH, Weinheim, **2008**, p. 3313; d) L. A. Saudan, *Acc. Chem. Res.* **2007**, *40*, 1309–1319.

[5] The initial isomer ratio of geranial to neral in **1** was maintained and consistent with that of geraniol to nerol in **2**, showing that no isomerization occurred.

[6] PtNPs, PdNPs, RhNPs, and RuNPs on CeO_2 were not effective even under much milder conditions. See the Supporting Information for details.
[7] See Supporting Information for details.
[8] Reported heterogeneous catalysts for the chemoselective reduction of **1** using H_2: Au/Fe_2O_3 (conversion of **1**, 90%; selectivity for **2**, 95%),[8a] Ir/H-β-zeolite (98%, 90%),[8b] Ag/SiO_2 (100%, 77%),[8c] Ag^0-nanocolloid (93%, 72%),[8d] $PtRu_5Sn/MgO$ (100%, 88%),[8e] and Au/*meso*-CeO_2 (>99%, 92%);[8f] a) C. Milone, M. L. Tropeano, G. Gulino, G. Neri, R. Ingoglia, S. Galvagno, *Chem. Commun.* **2002**, 868–869; b) M. De Bruyn, S. Coman, R. Bota, V. I. Parvulescu, D. E. De Vos, P. A. Jacobs, *Angew. Chem.* **2003**, *115*, 5491–5494; *Angew. Chem. Int. Ed.* **2003**, *42*, 5333–5336; c) M. Steffan, A. Jakob, P. Claus, H. Lang, *Catal. Commun.* **2009**, *10*, 437–441; d) P. G. N. Mertens, P. Vandezande, X. Ye, H. Poelman, I. F. J. Vankelecom, D. E. De Vos, *Appl. Catal A.* **2009**, *355*, 176–183; e) K. J. Uffalussy, B. K. Captain, R. D. Adams, A. B. Hungria, J. R. Monnier, M. D. Amiridis, *ACS Catal.* **2011**, *1*, 1710–1718; f) M.-M. Wang, L. He, Y.-M. Liu, Y. Cao, H.-Y. He, K.-N. Fan, *Green Chem.* **2011**, *13*, 602–607.

Received: November 21, 2012
Published online: March 15, 2013

